Protein Expression and Purification 201 (2023) 106172

Contents lists available at ScienceDirect

Protein Expression and Purification

journal homepage: www.elsevier.com/locate/yprep

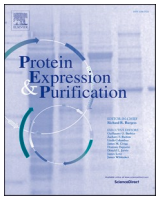

How to study a highly toxic protein to bacteria: A case of voltage sensor domain of mouse sperm-specific sodium/proton exchanger

César Arcos-Hernández [a], Esteban Suárez-Delgado [b], León D. Islas [b], Francisco Romero [a], Ignacio López-González [a], Hui-wang Ai [c], Takuya Nishigaki [a,*]

[a] Departamento de Genética del Desarrollo y Fisiología Molecular, Instituto de Biotecnología. Universidad Nacional Autónoma de México, Cuernavaca, Morelos, 62210, Mexico
[b] Departamento de Fisiología, Facultad de Medicina, Universidad Nacional Autónoma de México, Ciudad de México, 04510, Mexico
[c] Center for Membrane and Cell Physiology, Department of Molecular Physiology and Biological Physics, University of Virginia, Charlottesville, VA, 22908, USA

ARTICLE INFO

Keywords:
Heterologous expression
Toxic gene
Amber suppression
Intron insertion
Voltage-sensing domain

ABSTRACT

Heterologous expression systems have been used as a powerful experimental strategy to study the function of many proteins, particularly ion transporters. For this experiment, it is fundamental to prepare an expression vector encoding a protein of interest. However, we encountered problems in vector preparation of the voltage sensor domain (VSD) of murine sperm-specific Na^+/H^+ exchanger (sNHE) due to its severe toxicity to bacteria. We overcame the problems by insertion of an amber stop codon or a synthetic intron into the coding sequence of the VSD in the expression vectors. Both methods allowed us to express the protein of interest in HEK293 cells (combined with a stop codon suppression system for amber codon). The VSD of mouse sNHE generates voltage-dependent outward ionic currents, which is a probable cause of toxicity to bacteria. We propose these two strategies as practical solutions to study the function of any protein toxic to bacteria.

1. Introduction

The sperm-specific sodium/proton exchanger (sNHE) is an essential protein for male fertility, at least in mouse and human, because mutations in this exchanger cause male infertility due to severe problems in sperm flagellar beating [1,2]. Unlike other sodium/proton exchangers, sNHE (encoded by SLC9C) contains a voltage sensor domain (VSD) commonly found in voltage-dependent ion channels (Fig. 1A). Despite the importance of sNHE in sperm motility regulation, the characterization of the mammalian sNHE has not advanced because functional expression of the sNHE in heterologous systems has not been established [3].

In this study, we tried to characterize the VSD of mouse sNHE using the isolated VSD instead of the entire protein. In the course of our project, we encountered severe problems in preparation of expression vectors due to toxic effects of the VSD to *E. coli*. There are different strategies to avoid a gene's toxicity when preparing an expression vector [4]: changing the temperature during growing of transformed bacteria to reduce the copy number of the plasmid, selection of different promoters to control transcription strictly, usage of distinct *E. coli* strains to reduce expression of the toxic protein, and modification of the protein that reduce or eliminates the toxicity of the protein such as insertion of an intein, self-catalytic protein splicing element. On this matter, for a fungi calcium channel, CCH1, it was known to be impossible to prepare an expression vector in *E. coli* due to high toxicity. In 2009, a group developed a method that allowed them to clone the gene in yeast using a homologous recombination-based strategy [5]. Although the strategy was successful, it requires yeast and elaborated preparations of an insert and a vector to fuse them in vivo. Taking this example into account, it is desirable to establish an easy and efficient method that allows us to characterize this type of proteins.

In summary, we employed two distinct strategies to overcome the toxicity of the VSD in *E. coli*. 1) insertion of an amber stop codon into the toxic gene and its suppression upon protein expression, 2) insertion of an intron into the toxic gene and expression of the entire protein in eukaryotic cells where a splicing system exists. We believe that our report is a successful example of how one can study a protein that is highly toxic to *E. coli*. Also, our work could be of special interest for

Abbreviations: sNHE, sperm-specific sodium/proton exchanger; VSD, voltage sensor domain.

* Corresponding author.
E-mail address: takuya.nishigaki@ibt.unam.mx (T. Nishigaki).

https://doi.org/10.1016/j.pep.2022.106172
Received 29 June 2022; Received in revised form 30 August 2022; Accepted 9 September 2022
Available online 15 September 2022

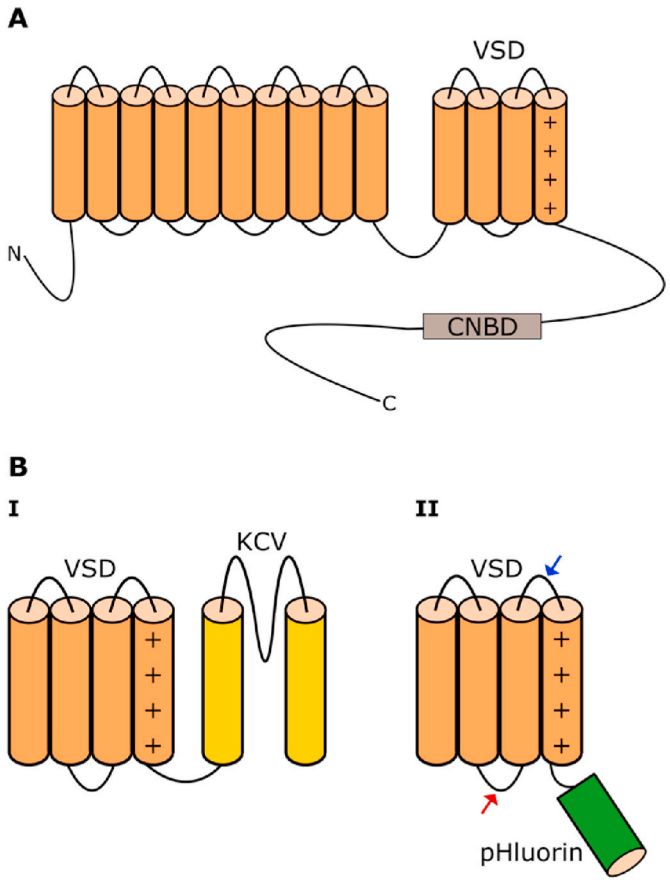

Fig. 1. Structure of sNHE and chimeric proteins with a mouse VSD of sNHE. (A) Mouse sNHE consists of 14 predicted transmembrane segments (S1–S14). The first ten segments form an ion exchanger (Na^+/H^+). The last four segments form a voltage-sensing domain (VSD). The long cytoplasmic C-terminus contains a cyclic nucleotide-binding domain (CNBD). (B) We designed two chimeric constructions: One fused to Kcv viral K^+ channel (I) and the other fused to pHluorin fluorescent protein (II). We prepared two versions of the second chimeric construction, one with a mutation of a tyrosine to an amber stop codon (blue arrow) and the other with an inserted intron (red arrow).

people studying voltage sensitive proteins difficult to clone in *E. coli*.

2. Materials and methods

The following DNA polymerases: Platinum SuperFi, Platinum Pfx (both from Thermo Fisher Scientific) and Vent (New England Biolabs) were used throughout the project. All restriction enzymes and pJET1.2 were from Thermo Fisher Scientific. The plasmids used in this study: pCAGEN was a gift from Connie Cepko (Addgene plasmid # 11160) [6], ArcLight-Q239 (in pCS2+) was a gift from Vincent Pieribone (Addgene plasmid # 36856) [7] and KvSynth1-GFP.pcDNA3 (Ci-VSP VSD) was a gift from Dr. Sandra M. Bajjalieh (University of Washington, Seattle). CMV-LUC2CP/intron/ARE was a gift from Gideon Dreyfuss (Addgene plasmid # 62858). All oligonucleotides for PCR primers were synthesized in the DNA synthesis and sequence unit of our institute and their sequences are described in Supplementary Table 1.

2.1. Cloning of the VSD of mouse sNHE ($msNHE_{VSD}$)

Total RNA was isolated from CD1 mouse testicle tissue using TRIzol Reagent (Thermo Fisher Scientific). A cDNA fragment containing the VSD of mouse sNHE ($msNHE_{VSD}$) was obtained by RT-PCR (PCR1 using 1F and 1R primers described in Supplementary Table 1). An amplified DNA fragment was cloned into pJET1.2 vector (Thermo Fisher Scientific) to obtain pJET1.2-$msNHE_{VSD}$. DNA sequences of open reading frames of all plasmids used in this study were determined in the DNA synthesis and sequence unit in our institute.

2.2. Preparation of expression vectors

2.2.1. *pCAGEN-$msNHE_{VSD}$-Kcv-GFP*

A plasmid KvSynth1-GFP.pcDNA3 encodes the VSD of Ci-VSP ($CiVSP_{VSD}$) fused to viral K^+ channel (Kcv) and GFP [8]. This plasmid produces a synthetic voltage-gated K^+ channel in mammalian cells [8, 9]. The open reading frame ($CiVSP_{VSD}$-Kcv-GFP) of this plasmid was amplified by PCR2 using 2F and 2R as primers (Supplementary Table 1). The amplified DNA fragment was inserted into pCAGEN [6] using EcoRI and NotI as cloning sites. The obtained plasmid (pCAGEN-$CiVSP_{VSD}$-Kcv-GFP) expressed higher amount of the synthetic K^+ channel in HEK293 cells than KvSynth1-GFP.pcDNA3 (data not shown). In order to obtain a chimeric protein containing VSD of mouse sNHE ($msNHE_{VSD}$), Kcv and GFP, we first amplified a DNA fragment encoding $msNHE_{VSD}$ by PCR3 using pJET1.2-$msNHE_{VSD}$ as a template and 3F and 3R as primers (Supplementary Table 1). Subsequently, Kcv-GFP region of cDNA was amplified by PCR4 using pCAGEN-$CiVSP_{VSD}$-Kcv-GFP as a template and 4F and 4R as primers (Supplementary Table 1). These two PCR products were digested with LguI (Type IIs restriction enzyme) and ligated with T4 ligase [10]. The ligated product was amplified by PCR5 with 3F and 4R primers and inserted into pCAGEN using EcoRI and NotI as cloning sites (pCAGEN-$msNHE_{VSD}$-Kcv-GFP as an expected plasmid). Supplementary Fig. 1 summarizes all procedures.

2.2.2. *pCS2+-$msNHE_{VSD}$-pHluorin*

The VSD of mouse sNHE ($msNHE_{VSD}$) was amplified by PCR6 using pJET1.2-$msNHE_{VSD}$ as a template and 6F and 6R primers (Supplementary Table 1). The amplified DNA was used to replace the VSD of the plasmid encoding ArcLight-Q239 (in pCS2+) [7] using HindIII and BamHI as cloning sites. The obtained plasmid (pCS2+-$msNHE_{VSD}$--pHluorin) encodes the VSD of mouse sNHE fused with pHluorin (Supplementary Fig. 2).

2.2.3. *pCS2+-$VSD_{Y665Amber}$-pHluorin*

Using pJET1.2-$msNHE_{VSD}$ as a template, the sequence TAC that encodes Tyrosine 665 of the VSD of mouse sNHE was replaced by an amber stop codon (TAG) by PCR-based mutagenesis [11] using 7F and 7R as primers (PCR7 Supplementary Table 1). After confirming the correct insertion of the amber stop codon by DNA sequencing, this plasmid (pJET1.2-$VSD_{Y665Amber}$) was used as a template and a DNA fragment containing the VSD with Y665Amber mutation ($VSD_{Y665Amber}$) was amplified by PCR8 with 6F and 6R primers. The amplified DNA was used to replace the VSD of the plasmid encoding ArcLight-Q239 (in pCS2+) using HindIII and BamHI as cloning sites. The obtained plasmid (pCS2+-$VSD_{Y665Amber}$-pHluorin) encodes $msNHE_{VSD}$ with Y665Amber mutation fused with pHluorin (Supplementary Fig. 2).

2.2.4. *pCS2+-VSD_{Intron}-pHluorin*

A small (133 bp) chimeric intron (from β-Globin and IgG) [12] was introduced into AG and G bases that encodes for the cytoplasmic loop between the second (S2) and the third (S3) transmembrane segments of the VSD of mouse sNHE (Fig. 1 and Fig. S2). To insert the intron within $msNHE_{VSD}$ (VSD_{Intron}), we amplified three DNA fragments by PCR that contain one or two LguI site(s). The first fragment (the N-terminal half of $msNHE_{VSD}$) was amplified by PCR9 using pJET1.2-$msNHE_{VSD}$ as template and 6F and 9R as primer (Supplementary Table 1). The second fragment (Intron) was amplified by PCR10 using CMV-LUC2CP/intron/ARE as template and 10F and 10R primers (Supplementary Table 1). The third fragment (the C-terminal half of $msNHE_{VSD}$) was amplified by PCR11 using pJET1.2-$msNHE_{VSD}$ as a template and 11F and 6R as primers (Supplementary Table 1). Thereafter, all three PCR products were digested by LguI and ligated. The

ligated product (VSD_{Intron}) was amplified by PCR12 using 6F and 6R primers and used to replace the VSD of ArcLight-Q239 (in pCS2+) to obtain pCS2+-VSD_{Intron}-pHluorin using HindIII and BamHI as cloning sites again (Supplementary Fig. 2).

2.2.5. Cell culture and transfection

The human embryonic kidney 293 (HEK293) cell line was maintained in Dulbecco's Modified Eagle Medium (DMEM) supplemented with 10% fetal bovine serum and antibiotic (Streptomycin (10,000 μg/ml) and Penicillin (100 U/ml))/antimycotic (Amphotericin B (25 μg/ml)) (all from Gibco) at 37 °C in a 4% CO_2 atmosphere. Transient expression was achieved by transfection of plasmid DNA using jetPEI (Polyplus). When the cells were transfected with pCS2+-$VSD_{Y665Amber}$-pHluorin and pMAH-MYRS, DMEM medium was supplemented with 1 mM L-Tyrosine until the experiment was performed.

2.2.6. Electrophysiology

The cells were used for experiments at 24 or 48 h after transfection. For voltage-clamp experiments using the whole-cell patch-clamp configuration, we used the following internal solution in mM: 133 NMDG-methanesulfonate, 5 NMDG-Cl (or 138 NMDG-Cl), 0.2 $MgCl_2$, 10 EGTA and 10 HEPES. The external solution contained in mM: 140 NMDG-Cl (or 140 NMDG-methanesulfonate), 3 KCl, 5 $CaCl_2$, 10 HEPES and 5 Glucose. The pH of the media was adjusted to 7.4 with NMDG. For macroscopic current recordings, we used a voltage step protocol from −80 to 80 mV in 10 mV increments, from a holding potential of −80 mV (or −120 mV). The borosilicate pipettes used for recordings, ranged in resistance from 3 to 7 MΩ. Ionic current recordings were sampled at 20 kHz and filtered at 5 kHz (four-pole Bessel filter), using an Axopatch 200B amplifier and the Axon 1550B digitizer (Molecular Devices). Linear capacitative currents were minimized analogically using the capacitative transient cancellation feature of the amplifier. For ion current recordings, online leak subtraction was applied using a p/-4 protocol. Stimulation, data acquisition and data analysis were done using pClamp software 11 (Molecular Devices).

2.2.7. Visualization of protein expression using fluorescence microscopy

The expression of all chimeric proteins (assessed by pHluorin's fluorescence) was confirmed using epifluorescence or confocal microscopy. In both cases, the cells were observed 24 or 48 h after transfection. In the case of confocal microscopy, the cells were grown, transfected, and observed in glass bottom dishes (Cat. FD35-100 from FluoroDish); the excitation wavelength was 488 nm using an objective lens 60× amplification in an Olympus IX81 inverted confocal microscope (these observations were done at the National Laboratory of Advanced Microscopy in our institute). Epifluorescence microscopy was performed during the electrophysiological experiments; the previously transfected cells were detached from the dishes using trypsin (TrypLE Express Enzyme (1X) Cat.12604–54 from Gibco), placed onto small glass pieces and observed under the microscope.

2.3. Results and discussion

2.3.1. Expression vectors of the VSD of mouse sNHE

It was previously demonstrated that hyperpolarized membrane potential (V_m) activates Na^+/H^+ exchange through the VSD of sNHE using the sea urchin ortholog expressed in CHO cells [13]. In this study, we decided to investigate the isolated VSD of mouse sNHE taking advantage of its modular nature [14]. In general, a VSD functions independently of other domains such as the pore domain of ion channels and the phosphatase of the voltage-sensitive lipid phosphatase (VSP) [15]. For example, the VSD of Ci-VSP maintains its function after being fused to a viral K^+ channel [9,16] or to a fluorescent protein [7]. According to these previous reports, we designed two chimeric proteins by fusing the VSD to the viral K^+ channel (Kcv) or the fluorescent protein (pHluorin) (Fig. 1B).

However, we encountered severe problems in preparation of the plasmids that encode the VSD of mouse sNHE ($msNHE_{VSD}$). Actually, we have never obtained a desired plasmid encoding the $msNHE_{VSD}$ connected to the Kcv channel (pCAGEN-$msNHE_{VSD}$-Kcv-GFP). Namely, we obtained a quite small number of colonies of *E. coli* after transformation. All plasmids we prepared from those *E. coli* colonies were smaller than expected (Fig. S3A) with a significant deletion of DNA (Fig. S3B).

On the other hand, in the very first preparation of a plasmid encoding $msNHE_{VSD}$ connected to pHluorin (pCS2+-$msNHE_{VSD}$-pHluorin) using JM109(DE3), we obtained one colony that encodes the correct coding sequence. We confirmed that HEK293 cells transfected with this plasmid exhibit fluorescence signals of pHluorin although the protein did not localize preferentially at the plasma membrane as ArcLight (a VSD of Ci-VSP fused to pHluorin) does (Fig. S4). Considering that some VSDs themselves can form ion channels [17–19], we suspected that $msNHE_{VSD}$ might form an ion channel. Actually, we recorded voltage-dependent outward currents from a cell transfected with the plasmid pCS2+-$msNHE_{VSD}$-pHluorin (Fig. S5). We wanted to repeat this experiment, but we couldn't because we failed to obtain any new *E. coli* colonies transformed with this plasmid. Therefore, we tried to obtain the same plasmid construct repeating the same procedure, but we obtained only plasmids with mutated inserts (Fig. S6). Thereafter, we tried other *E. coli* strains, incubation in low temperatures or other plasmid vectors [4]. However, all our efforts to recover the plasmid fell in vain. Therefore, we reasoned that the problems might be caused by a severe toxic effect of $msNHE_{VSD}$ on *E. coli*. To overcome this problem, we tried two distinct strategies that eliminate the gene toxicity during *E. coli* transformation.

2.3.2. Amber stop codon insertion and its suppression

We first used the amber stop codon suppression system. In the last two decades, significant technical advances have been made to incorporate unnatural amino acids into a recombinant protein [20–23]. This technology is based on the stop codon suppression system, where a particular amino acid can be incorporated into a certain stop codon in the presence of an orthogonal aminoacyl-tRNA synthetase/tRNA pair. However, without the stop codon suppression system, a recombinant protein will not be produced in transfected cells. Actually, a stop codon insertion has been used for preparation of expression vector encoding some toxic proteins such as Ndd protein of T4 bacteriophage and barnase (RNase of bacteria) [24,25]. These proteins were expressed in bacteria and in plants using stop codon suppression systems. However, this strategy has been used to regulate gene expression of functionally known protein, not for analysis of biochemical or biophysical properties of an uncharacterized protein. We introduced an amber stop codon at the position 665 of mouse sNHE, originally occupied by a tyrosine ($VSD_{Y665Amb}$) (Fig. 2A and Fig. S7A). As expected, we were able to prepare the desired plasmid (pCS2+-$VSD_{Y665Amb}$-pHluorin) without any problems (Fig. 2B). To suppress the amber stop codon in HEK293 cells, we co-transfected with a pMAH-MYRS plasmid that encodes an aminoacyl-tRNA synthetase/tRNA pair (Fig. S7B). pMAH-MYRS incorporates 3-nitro-L-tyrosine (3-NY) into the amber stop codon in mammalian cells, but also incorporates tyrosine in the presence of additional tyrosine (mM range) in the medium. We described the pMAH plasmid backbone previously [21], while 3-NY-aminoacyl-tRNA synthetase is different from the wild-type enzyme by only two mutations (Y37L/Q195S) (Fig. S7C). Detailed characterization and other applications of pMAH-MYRS will be reported elsewhere. Using this method, we were able to produce the complete chimeric protein ($msNHE_{VSD}$ – pHluorin) in HEK293 cells (Fig. 2C). In contrast, we observed negligible fluorescence in HEK293 cells transfected only with pCS2+-$VSD_{Y665Amb}$-pHluorin (Fig. 2C), indicating that amber stop codon can be suppressed only by co-transfection with pMAH-MYRS. Furthermore, we detected voltage-dependent outward currents from the co-transfected HEK293 cells (Fig. 2D). As a control we transfected HEK293 cells with ArcLight Q239 (the VSD of Ci-VSP fused to pHluorin)

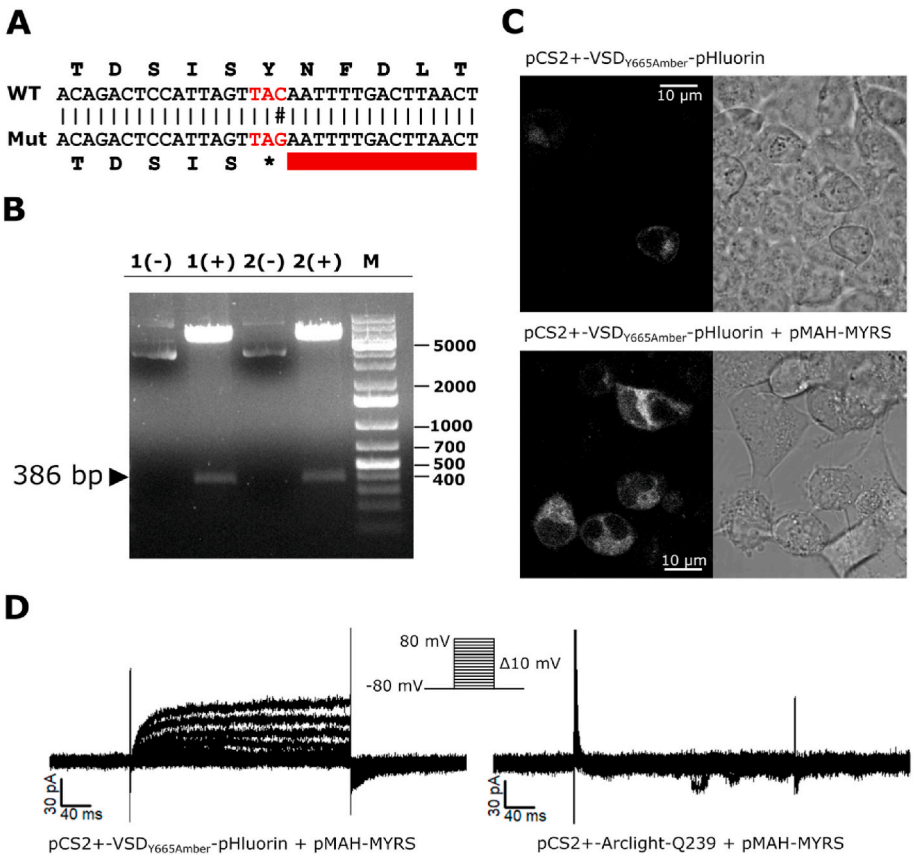

Fig. 2. Plasmid encoding msNHE$_{VSD}$-pHluorin with amber stop codon and its suppression in HEK293 cells.
(A) Partial DNA and amino acid sequence of pCS2+-VSD$_{Y665Amber}$-pHluorin. Amber stop codon (TAG) inserted in Y665 (TAC) is highlighted in red. (B) Gel electrophoresis pattern of two plasmids, both corresponding to pCS2+-VSD$_{Y665Amber}$-pHluorin. The lanes contain the plasmids before (−) and after (+) digestion with HindIII and BamHI. The expected size of the insert (386 bp arrow) was observed after digestion. (C) Confocal fluorescence (left) and bright field (right) images of HEK293 cells transfected only with pCS2+-VSD$_{Y665Amber}$-pHluorin (top) or co-transfected with pMAH-MYRS with 1 mM Tyrosine (bottom). Scale bar, 10 μm. (D) Voltage-clamp recordings of HEK293 cells transfected with pCS2+-VSDY665Amber-pHluorin (left) or pCS2+-Arclight Q239 (right). In both cases, HEK293 cells were co-transfected with pMAH-MYRS. The currents were obtained using a step protocol from −80 to +80 mV from a holding potential of - 80 mV. The mean current density at +60 mV for pCS2+-VSDY665Amber-pHluorin cells was: 5.7 ± 1.8 pA/pF (n = 5).

and pMAH-MYRS, but the cells did not produce any detectable ionic current (Fig. 2D). Currently, a stop codon suppression system is mainly used for insertion of unnatural amino acids. However, we used this technique to produce an intact protein in eukaryotic cells, which is an unconventional, but quite useful, technique to overcome the problem of a toxic protein to bacteria.

In this study, we used an amber insertion strategy to purify the plasmid encoding a toxic msNHE$_{VSD}$ gene from *E. coli*, and did not intend to regulate the expression level of msNHE$_{VSD}$-pHluorin in HEK293 cells using the amber suppression system. In the future, we may use an amber suppression system without background readthrough in mammalian cells, and then use unnatural amino acid to regulate the expression of the full-length protein. We expect that such controlled expression strategy may serve to study time-resolved cell responses to a protein of interest.

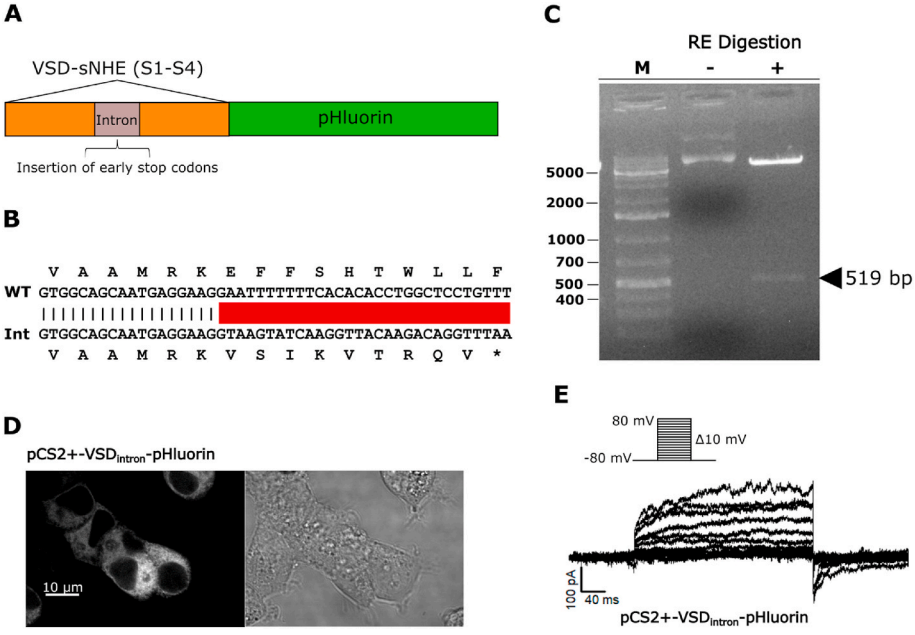

Fig. 3. Insertion of a small intron in msNHE$_{VSD}$ and expression of the msNHE$_{VSD}$-pHluorin in HEK293 cells.
(A) A small synthetic intron was inserted in the middle of msNHE$_{VSD}$ gene in order to prevent the entire protein expression in bacteria. (B) Partial DNA and amino acid sequences of WT and intron-inserted msNHE$_{VSD}$. The later produces a truncated protein with unrelated 9 amino acids in the C-terminus (represented by the red bar). (C) Gel electrophoresis pattern of pCS2+-VSD$_{Intron}$-pHluorin before (−) and after (+) digestion with HindIII and BamHI. The expected size of the insert DNA (519 bp) was observed after digestion. (D) Confocal images showing pHluorin fluorescence (left) and bright field (right) of HEK293 cells transfected with pCS2+-VSD$_{Intron}$-pHluorin. Scale bar, 10 μm. (E) Voltage clamp recording of a HEK293 cell transfected with pCS2+-VSD$_{Intron}$-pHluorin. The currents were obtained using a step protocol from −80 to +80 mV from a holding potential of −80 mV. The mean current density at +60 mV was 13.2 ± 2.2 pA/pF (n = 5).

2.3.3. Intron insertion

Several viral proteins are toxic to bacteria and plasmids containing such gene are hard to amplify in *E. coli* [26]. To overcome this problem, Johansen reported in 1996 that insertion of intron(s) into cDNA of plant potyvirus facilitated plasmid amplification in *E. coli* and allowed the identical potyvirus production in plant leaves transfected with such plasmids [27]. Afterwards, intron insertion was employed in several viral proteins toxic to *E. coli* [28–30]. Although this method is theoretically relevant for any protein regardless of the origin of organisms, it has been mainly used for viral proteins.

The amber stop codon suppression system was successful for expression of msNHE$_{VSD}$-pHluorin in HEK293 cells. However, it was quite hard to perform whole-cell patch-clamp recordings. In order to explore another method, we decided to try intron insertion as the second strategy to eliminate the VSD toxicity in bacteria. We introduced a small (133 base pairs) synthetic intron, which has at least one stop codon in any reading frame [12], into the cDNA that encodes msNHE$_{VSD}$ (Fig. 3A, Fig. S7B and Fig. S8A). In theory, bacteria produce a truncated VSD with extra 9 amino acids in its C-terminus (Fig. 3B). As expected, we were able to prepare a plasmid encoding msNHE$_{VSD}$ with the intron (pCS2+-VSD$_{Intron}$-pHluorin) without any problems (Fig. 3C).

HEK293 cells transfected with pCS2+-VSD$_{Intron}$-pHluorin expressed msNHE$_{VSD}$-pHluorin (Fig. 3D). The cells expressing msNHE$_{VSD}$-pHluorin with the intron system exhibited similar outward currents as observed previously (Fig. 3E). Furthermore, we recorded larger ionic currents with the intron system than those with the amber suppression system (Fig. S9). It is known that splicing enhances recombinant protein expression by mRNA accumulation [31]. On the other hand, the amber suppression system has to compete with translation termination. These distinct properties might explain the difference of the amplitudes of the outward ionic currents between the two methods. However, HEK293 transfected with pCS2-VSD$_{intron}$-pHluorin cells are still fragile compared to those transfected with ArcLight Q239, confirming that msNHE$_{VSD}$ is toxic to eukaryotic cells not only to bacteria.

3. Conclusion

Besides our case, there are some examples of transmembrane proteins that are toxic to bacteria by alteration of the membrane permeability: influenza M2 protein [32], the 6K protein [33] and the E protein from SARS coronavirus [34]. We revealed that msNHE$_{VSD}$ forms an ion channel in HEK293 cells, which is a probable cause of its toxicity to bacteria as well as HEK293 cells. In this study, it was more difficult to obtain a whole-cell patch-clamp recording with the stop codon suppression system than the intron system, probably because of an additional stress to HEK293 cells through the stop codon suppression. However, an amber stop codon insertion into a DNA fragment is technically much easier than intron insertion. Therefore, further trials with distinct proteins should be done to evaluate the stop codon suppression system to overcome the toxicity of any toxic genes to bacteria. We believe that our report promotes two strategies, i) stop codon suppression and ii) intron insertion, as practical solutions against the problem of any recombinant protein toxic to bacteria, which will allow the expression of the protein in eukaryotic cell to characterize its biochemical and biophysical properties.

We observed outward currents from the VSD of mouse sNHE expressed in HEK293 cells. However, this activity is probably an artifact of the isolation of the VSD from the sNHE because such currents were not reported from mouse spermatozoa [35]. As a similar case, an isolated VSD of shaker channel generates gating pore currents although the complete shaker channel does not generate such currents [18]. We need to characterize the entire mouse sNHE and the strategies we employed in this study should contribute to this purpose.

Contribution of authors

C. A. performed all experiments and analysis of data and wrote the manuscript preparing all figures. E.S. performed initial characterization of the VSD fused with pHluorin. L.I. designed the initial part of the chimeric construction and discussed all results. F.R. prepared cDNA encoding the VSD of mouse sNHE. I.L. supervised and discussed the electrophysiological recordings. H.W. provided the pMAH-MYRS plasmid. T.N. conceived the project and wrote the manuscript.

Authors have no conflicts of interest with the content of this article.

Acknowledgements

We thank Yoloxochitl Sánchez Guevara for all her technical supports for this project. We thank Gisela Edith Rangel Yescas for her technical support of initial phase of the project. We thank Jose Luis De la Vega and Paulina Torres for general maintenance of our laboratory. We thank Carmen Nina Pastor Colón for her technical support of the initial simulation of the VSD folding. We also thank Ana Yanci Alarcon, Abigail Roldan, Santiago Becerra, Eugenio Lopez, Jorge Yañez and Paul Gaytan of the synthesis and sequencing unit for the preparation of oligonucleotides and plasmid sequencing. Finally, we thank Arturo Pimentel and Veronica Rojo of the National Laboratory of Advanced Microscopy for the support during the confocal imaging acquisition.

This work was supported by CONACyT (CB2017-2018 A1-S-8768), PAPIIT (DGAPA IN205719 and IN205722), UC MEXUS-CONACyT (CN-16-56) to TN, PAPIIT (DGAPA IN208321) to ILG, PAPIIT (DGAPA IN215621) to LDI and Japan Society for the Promotion of Science's Core-to-Core Program, and White Rock Foundation.

Appendix A. Supplementary data

Supplementary data to this article can be found online at https://doi.org/10.1016/j.pep.2022.106172.

References

[1] D. Wang, S.M. King, T. a Quill, L.K. Doolittle, D.L. Garbers, A new sperm-specific Na+/H+ exchanger required for sperm motility and fertility, Nat. Cell Biol. 5 (12) (2003) 1117–1122, https://doi.org/10.1038/ncb1072.

[2] E. Cavarocchi, et al., The sodium/proton exchanger SLC9C1 (sNHE) is essential for human sperm motility and fertility, Clin. Genet. (2021), https://doi.org/10.1111/cge.13927. October 2020.

[3] D. Wang, et al., A sperm-specific Na+/H+ exchanger (sNHE) is critical for expression and in vivo bicarbonate regulation of the soluble adenylyl cyclase (sAC), Proc. Natl. Acad. Sci. U.S.A. 104 (22) (2007) 9325–9330, https://doi.org/10.1073/pnas.0611296104.

[4] F. Saida, M. Uzan, B. Odaert, F. Bontems, Expression of highly toxic genes in E. coli: special strategies and genetic tools, Curr. Protein Pept. Sci. 7 (1) (2006) 47–56, https://doi.org/10.2174/138920306775474095.

[5] K. Vu, J. Bautos, M.P. Hong, A. Gelli, The functional expression of toxic genes: lessons learned from molecular cloning of CCH1, a high-affinity Ca2+ channel, Anal. Biochem. 393 (2) (2009) 234–241, https://doi.org/10.1016/j.ab.2009.06.039.

[6] T. Matsuda, C.L. Cepko, Electroporation and RNA interference in the rodent retina in vivo and in vitro, Proc. Natl. Acad. Sci. U.S.A. 101 (1) (2004) 16–22, https://doi.org/10.1073/pnas.2235688100.

[7] L. Jin, Z. Han, J. Platisa, J.R.A. Wooltorton, L.B. Cohen, V.A. Pieribone, Single action potentials and subthreshold electrical events imaged in neurons with a fluorescent protein voltage probe, Neuron 75 (5) (2012) 779–785, https://doi.org/10.1016/j.neuron.2012.06.040.

[8] M.G. Rosasco, S.E. Gordon, S.M. Bajjalieh, Characterization of the functional domains of a mammalian voltage-sensitive phosphatase, Biophys. J. 109 (12) (2015) 2430–2491, https://doi.org/10.1016/j.bpj.2015.11.004.

[9] C. Arrigoni, I. Schroeder, G. Romani, J.L. Van Etten, G. Thiel, A. Moroni, The voltage-sensing domain of a phosphatase gates the pore of a potassium channel, J. Gen. Physiol. 141 (3) (2013) 389–395, https://doi.org/10.1085/jgp.201210940.

[10] I. Kotera, T. Nagai, A high-throughput and single-tube recombination of crude PCR products using a DNA polymerase inhibitor and type IIS restriction enzyme, J. Biotechnol. 137 (1–4) (2008) 1–7, https://doi.org/10.1016/j.jbiotec.2008.07.1816.

[11] L. Zheng, U. Baumann, J. Reymond, An efficient one-step site-directed and site-saturation mutagenesis protocol, Nucleic Acids Res. 32 (14) (2004), https://doi.org/10.1093/nar/gnh110.

[12] I. Younis, M. Berg, D. Kaida, K. Dittmar, C. Wang, G. Dreyfuss, Rapid-response splicing reporter screens identify differential regulators of constitutive and alternative splicing, Mol. Cell Biol. 30 (7) (2010) 1718–1728, https://doi.org/10.1128/mcb.01301-09.
[13] F. Windler, et al., The solute carrier SLC9C1 is a Na+/H+-exchanger gated by an S4-type voltage-sensor and cyclic-nucleotide binding, Nat. Commun. 9 (1) (2018) 1–13, https://doi.org/10.1038/s41467-018-05253-x.
[14] Y. Okamura, Y. Okochi, Molecular mechanisms of coupling to voltage sensors in voltage-evoked cellular signals, Proc. Japan Acad. Ser. B Phys. Biol. Sci. 95 (3) (2019) 111–135, https://doi.org/10.2183/PJAB.95.010.
[15] Y. Murata, H. Iwasaki, M. Sasaki, K. Inaba, Y. Okamura, Phosphoinositide phosphatase activity coupled to an intrinsic voltage sensor, Nature 435 (7046) (2005) 1239–1243, https://doi.org/10.1038/nature03650.
[16] S. Gazzarrini, et al., The viral potassium channel Kcv : structural and functional features, FEBS Lett. 552 (2003) 12–16, https://doi.org/10.1016/S0014-5793(03)00777-4.
[17] H. Arima, H. Tsutsui, Y. Okamura, Conservation of the Ca 2+ -permeability through the voltage sensor domain of mammalian catsper subunit, Channels 12 (1) (2018) 240–248, https://doi.org/10.1080/19336950.2018.1476791.
[18] J. Zhao, R. Blunck, The isolated voltage sensing domain of the Shaker potassium channel forms a voltage-gated cation channel, Elife 5 (2016) 1–18, https://doi.org/10.7554/eLife.18130. OCTOBER2016.
[19] K.A. Sutton, M.K. Jungnickel, L. Jovine, H.M. Florman, Evolution of the voltage sensor domain of the voltage-sensitive phosphoinositide phosphatase VSP/TPTE suggests a role as a proton channel in eutherian mammals, Mol. Biol. Evol. 29 (9) (2012) 2147–2155, https://doi.org/10.1093/molbev/mss083.
[20] S.L. Hyun, J. Guo, E.A. Lemke, R.D. Dimla, P.G. Schultz, Genetic incorporation of a small, environmentally sensitive, fluorescent probe into proteins in Saccharomyces cerevisiae, J. Am. Chem. Soc. 131 (36) (2009) 12921–12923, https://doi.org/10.1021/ja904896s.
[21] A. Chatterjee, H. Xiao, M. Bollong, H.W. Ai, P.G. Schultz, Efficient viral delivery system for unnatural amino acid mutagenesis in mammalian cells, Proc. Natl. Acad. Sci. U.S.A. 110 (29) (2013) 11803–11808, https://doi.org/10.1073/pnas.1309584110.
[22] C.C. Liu, P.G. Schultz, Adding new chemistries to the genetic code, Annu. Rev. Biochem. 79 (2010) 413–444, https://doi.org/10.1146/annurev.biochem.052308.105824.
[23] D.D. Young, P.G. Schultz, Playing with the molecules of life, ACS Chem. Biol. 13 (4) (2018) 854–870, https://doi.org/10.1021/acschembio.7b00974.
[24] J.Y. Bouet, N.J. Campo, H.M. Krisch, J.M. Louarn, The effects on Escherichia coli of expression of the cloned bacteriophage T4 nucleoid disruption (ndd) gene, Mol. Microbiol. 20 (3) (1996) 519–528, https://doi.org/10.1046/j.1365-2958.1996.5411067.x.
[25] A.S. Betzner, M.P. Oakes, E. Huttner, Transfer RNA-mediated suppression of amber stop codons in transgenic Arabidopsis thaliana, Plant J. 11 (3) (1997) 587–595, https://doi.org/10.1046/j.1365-313X.1997.11030587.x.
[26] J.C. Boyer, A.L. Haenni, Infectious transcripts and cDNA clones of RNA viruses, Virology 198 (2) (1994) 415–426, https://doi.org/10.1006/viro.1994.1053.
[27] I.E. Johansen, Intron insertion facilitates amplification of cloned virus cDNA in Escherichia coli while biological activity is reestablished after transcription in vivo, Proc. Natl. Acad. Sci. U.S.A. 93 (22) (1996) 12400–12405, https://doi.org/10.1073/pnas.93.22.12400.
[28] J.J. López-Moya, J.A. García, Construction of a stable and highly infectious intron-containing cDNA clone of plum pox potyvirus and its use to infect plants by particle bombardment, Virus Res. 68 (2) (2000) 99–107, https://doi.org/10.1016/S0168-1702(00)00161-1.
[29] J.M. González, Z. Pénzes, F. Almazán, E. Calvo, L. Enjuanes, Stabilization of a full-length infectious cDNA clone of transmissible gastroenteritis coronavirus by insertion of an intron, J. Virol. 76 (9) (2002) 4655–4661, https://doi.org/10.1128/jvi.76.9.4655-4661.2002.
[30] J. Guo, et al., Stabilization of a full-length infectious cDNA clone for duck Tembusu virus by insertion of an intron, J. Virol. Methods 283 (June, 2020), https://doi.org/10.1016/j.jviromet.2020.113922.
[31] A. Nott, S.H. Meislin, M.J. Moore, A quantitative analysis of intron effects on mammalian gene expression, RNA 9 (5) (2003) 607–617, https://doi.org/10.1261/rna.5250403.
[32] L.H. Pinto, L.J. Holsinger, R.A. Lamb, Influenza virus M2 protein has ion channel activity, Cell 69 (3) (1992) 517–528, https://doi.org/10.1016/0092-8674(92)90452-I.
[33] M.A. Sanz, L. Pérez, L. Carrasco, Semliki forest virus 6K protein modifies membrane permeability after inducible expression in Escherichia coli cells, J. Biol. Chem. 269 (16) (1994) 12106–12110.
[34] Y. Liao, J. Lescar, J.P. Tam, D.X. Liu, Expression of SARS-coronavirus envelope protein in Escherichia coli cells alters membrane permeability, Biochem. Biophys. Res. Commun. 325 (1) (2004) 374–380, https://doi.org/10.1016/j.bbrc.2004.10.050.
[35] X.H. Zeng, B. Navarro, X.M. Xia, D.E. Clapham, C.J. Lingle, Simultaneous knockout of slo3 and catsper1 abolishes all alkalization- and voltage-activated current in mouse spermatozoa, J. Gen. Physiol. 142 (3) (2013) 305–313, https://doi.org/10.1085/jgp.201311011.

Supplementary Table 1. Information of PCR primers with nucleotide sequences

PCR1 for cloning of the VSD of mouse sNHE
1F: TCG GAC ATT TCT CTC GGT T
1R: TAT CTG CTG GCT CAT CCT T

PCR2 for subcloning of $CiVSP_{VSD}$-Kcv-GFP into pCAGEN plasmid
2F: CGC CGG AAT TCA CCA TGG AGG GAT TTG AC (EcoRI)
2R: GGA AAG GAC AGT GGG AGT GG

PCR3 for amplification of the VSD of mouse sNHE with RE sites
3F: GCG GGA ATT CAC CAT GGT CTT CAC AAA TGA (EcoRI)
3R: CGG CTC TTC TTT TGG TGT TAC AAG C (LguI)

PCR4 for amplification of the Kcv-GFP from pCAGEN-$CiVSP_{VSD}$-Kcv-GFP
4F: CCG CTC TTC CAA AAA TGT TAG TGT TTA GTA A (LguI)
4R: AGC CTG CAC CTG AGG A

PCR5 for amplification of the ligated product ($msNHE_{VSD}$-Kcv-GFP)
3F and 4R

PCR6 for amplification of the VSD of mouse sNHE for ArcLight-Q239 (pCS2+)
6F: CCC AAG CTT ACC ATG GTC TTC ACA AAT GAA TTT GAA TAT ACT GG (HindIII)
6R: CAC GGA TCC CCC AGT AGT TTT GGT GTT ACT AGC TTC AAG ATG CGC AG (BamHI).

PCR7 for site-specific mutagenesis of pJET1.2-$msNHE_{VSD}$ (Y665Amber)
7F: CCA TTA GTT AGA ATT TTG ACT TAA CTG AGA CTG TGG T
7R: CAA AAT TCT AAC TAA TGG AGT CTG TTT CGA TAA G

PCR8 for amplification of the $VSD_{Y665Amber}$
6F and 6R

PCR9 for amplification of the N-terminal half of $msNHE_{VSD}$
6F
9R: CCC GCT CTT CAC TTA CCT TCC TCA TTG CTG CCA CCT TAA (LguI)

PCR10 for amplification of intron
10F: CGG GCT CTT CTA AGT ATC AAG GTT ACA AGA CAG GTT TAA G (lguI)
10R: CCG CGT CTT CCT GTG GAG AGA AAG GCA AAG TGG A (LguI)

PCR11 for amplification of the C-terminal half of $msNHE_{VSD}$
11F: CCC GCT CTT CTA CAG GAA TTT TTT TCA CAC ACC TGG CTC (LguI)
6R

PCR12 for amplification of the VSD_{Intron}
6F and 6R

Fig. S1

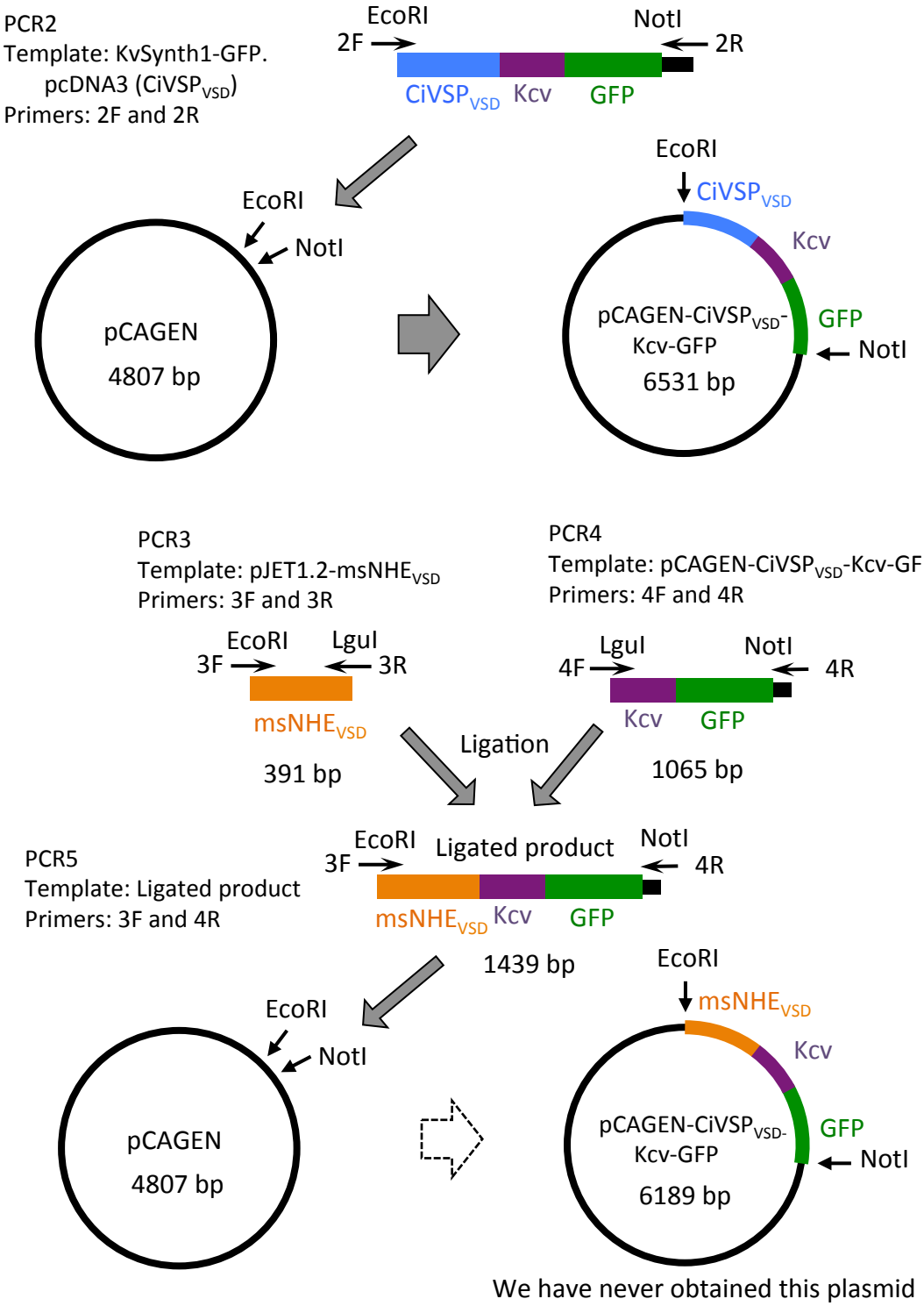

Figure S1. Procedure for preparation of pCAGEN-CiVSP$_{VSD}$-Kcv-GFP

Fig. S2

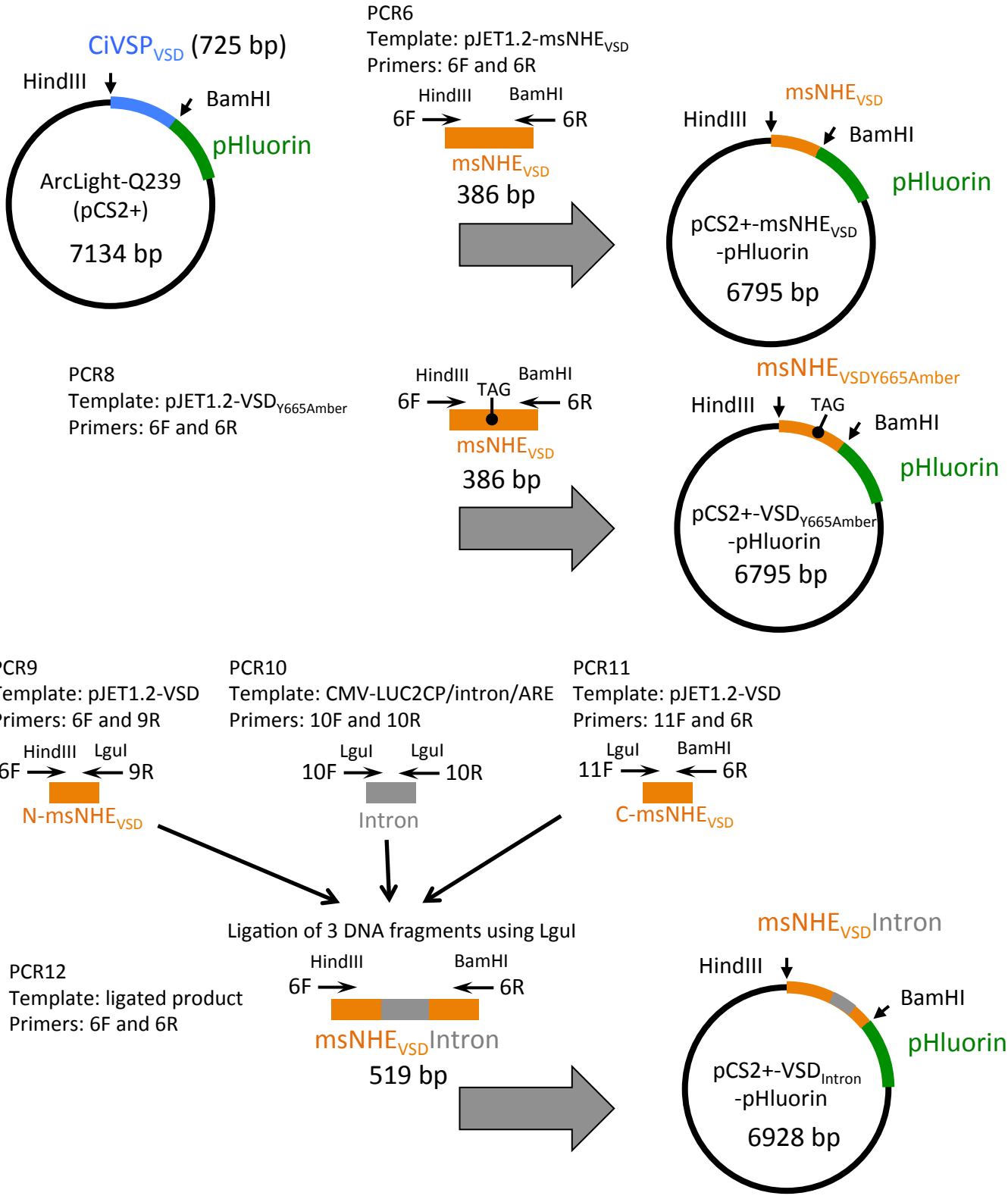

Figure S2. Procedure for pCS2+-msNHE$_{VSD}$-pHluroin and its derivatives

Fig. S3

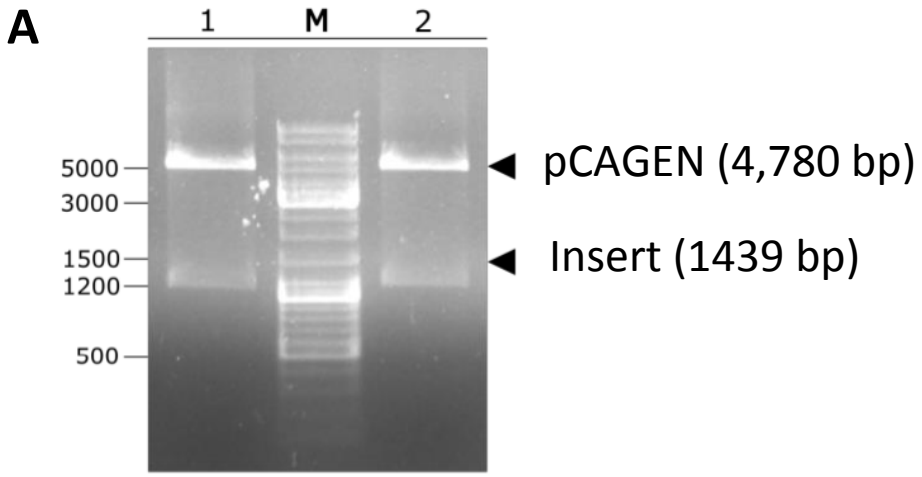

B

```
A.A.                                                        M  V  F  T
Expec.  AACGTGCTGGTTATTGTGCTGTCTCATCATTTTGGCAAAGAATTCACCATGGTCTTCACA  60
Obt.    AACGTGCTGGTTATTGTGCTGTCTCATCATTTTGGCAAAGAATTCACCATGGTCTTCA--  58
        ************************************************************
                  S1
A.A.     N  E  F  E  Y  T  G  Y  L  V  V  L  M  S  T  Y  P  M  I  I
Expec.  AATGAATTTGAATATACTGGATACCTTGTGGTATTAATGAGCACATATCCTATGATAATC 120
Obt.    ------------------------------------------------------------  58
                                                        S2
A.A.    C  W  I  S  R  L  K  D  I  Y  D  N  E  I  K  C  A  N  Y  Y
Expec.  TGTTGGATTTCCCGACTAAAAGACATCTATGACAACGAGATAAAATGTGCTAACTACTAT 180
Obt.    ------------------------------------------------------------  58

A.A.    F  L  A  F  Y  I  L  E  A  L  L  K  V  A  A  M  R  K  E  F
Expec.  TTTCTTGCCTTCTATATTCTAGAGGCTCTACTTAAGGTGGCAGCAATGAGGAAGGAATTT 240
Obt.    ------------------------------------------------------------  58
      S3
A.A.    F  S  H  T  W  L  L  F  E  L  G  I  T  L  V  G  I  L  D  I
Expec.  TTTTCACACACCTGGCTCCTGTTTGAGCTGGGGATTACCTTAGTCGGCATCCTAGATATA 300
Obt.    ------------------------------------------------------------  58
                                                        S4
A.A.    I  L  I  E  T  D  S  I  S  Y  N  F  D  L  T  E  T  V  V  F
Expec.  ATACTTATCGAAACAGACTCCATTAGTTACAATTTTGACTTAACTGAGACTGTGGTCTTC 360
Obt.    ------------------------------------------------------------  58

A.A.    M  N  V  I  R  L  L  R  I  L  R  I  L  K  L  V  T  P  K
Expec.  ATGAACGTGATTCGACTCCTTCGTATACTGCGCATCTTGAAGCTTGTAACACCAAAAT   418
Obt.    -CAAACGTGATTCGACTCCTTCGTATACTGCGCATCTTGAAGCTTGTAACACCAAAAT   115
           ************************************************************
```

Figure S3. Problems in pCAGEN-msNHE$_{VSD}$-Kcv-GFP preparation.
(A) Electrophoresis patterns of two putative plasmids (pCAGEN-msNHE$_{VSD}$-Kcv-GFP) in lanes 1 and 2 digested with EcoRI and NotI. Expected DNA size: 4780 bp for pCAGEN and 1439 bp for insert DNA. Lane M: DNA markers. (B) Sequences of expected amino acid (A.A.), expected DNA (Expec.) and obtained DNA (Obt.) are shown. Identical DNA sequences was indicated by asterisk. Four boxes indicate putative transmembrane domain (S1-S4) of VSD of mouse sNHE. The DNA region encoding S1-S3 of the VSD is missing in the obtained plasmid.

Fig. S4

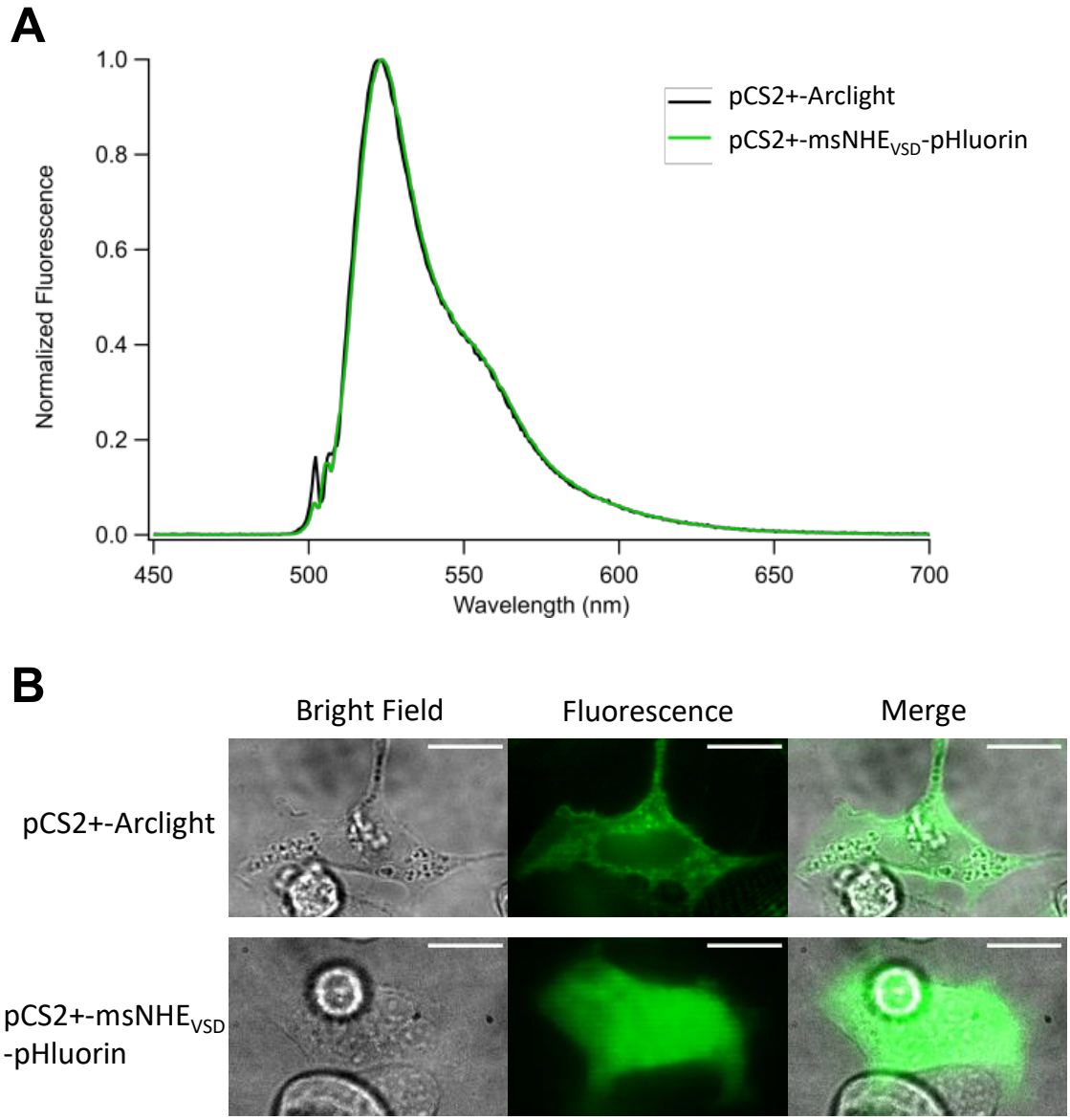

Figure S4. Fluorescence experiments of pCS2+-Arclight and pCS2+-msNHE$_{VSD}$-pHluorin expressed in HEK293 cells. (A) Emission spectrum of pCS2+-Arclight (black, n = 4) and pCS2+-msNHE$_{VSD}$-pHluorin (green, n = 3). The emission peak wavelength was around 523 nm in both signals. Spectrum centroid was 540.8 ± 0.3 nm and 541.3 ± 0.4 nm for each fusion protein, respectively. The emission spectra of the fluorescence images were determined by SpectraPro 2150i spectrograph (Princeton Instruments, USA) mounted between the microscope (Nikon TE 2000U with 60x oil immersion objective, NA 1.4) and a Ixon Ultra EMCCD camera (Andor, Oxford instruments, Ireland) controlled by Micromanager software. The excitation wavelength for the emission measurements was 488 nm. The spectra were recorded by measuring lines scans that involve the cell membrane and background were subtracted. (B) Fluorescence distribution of pCS2+-Arclight (upper panel) and pCS2+-msNHE$_{VSD}$-pHluorin (lower panel). Note that Arclight predominates in cell membrane whereas pCS2+-msNHE$_{VSD}$-pHluorin is also located intracellularly. Scale bar = 10 µm.

Fig. S5

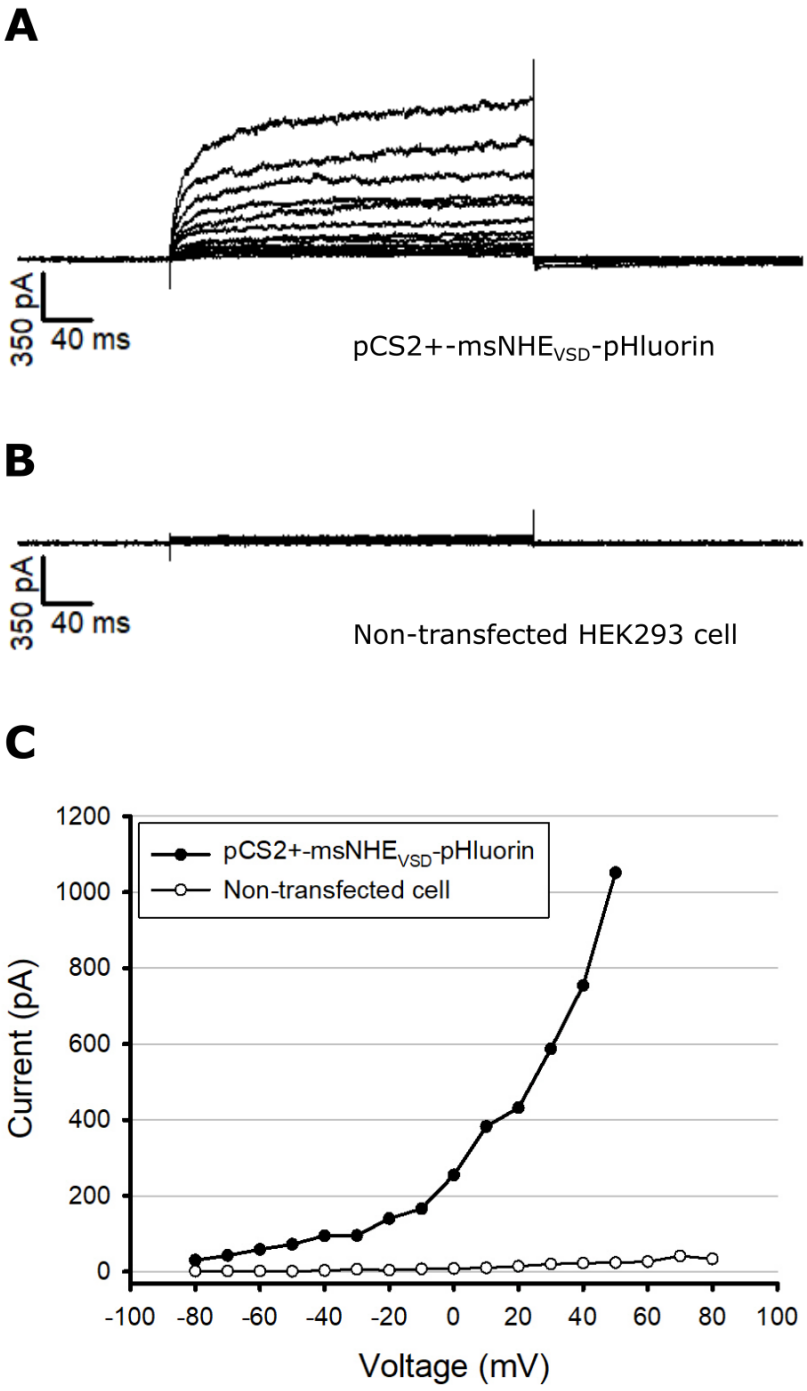

Figure S5. Ionic current recordings of pCS2+-msNHE$_{VSD}$-pHluorin. Voltage-clamp recordings of a HEK293 cell transfected with pCS2+-msNHE$_{VSD}$-pHluorin (A) or a non-transfected cell (B). In both cases the main ions in the internal and external solution were NMDG-Cl and NaCl respectively. (C) Current-voltage curve of the recordings shown in A and B. The currents were obtained using a step protocol from -80 to +80 mV from a holding potential of -120 mV.

Fig. S6

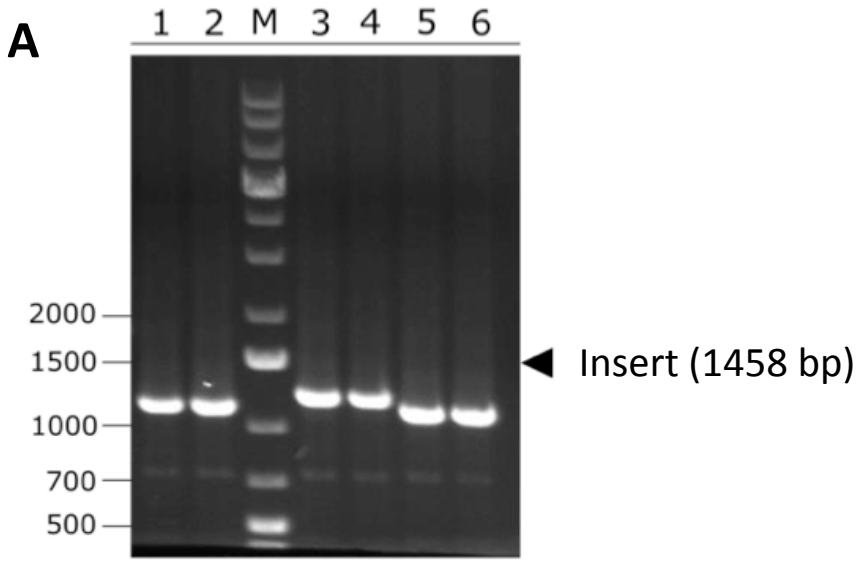

B

```
A.A.
Expec.  CGCCATTCTGCCTGGGGACGTCGGAGCTAGCTTGATTTAGGTGACACTATAGAATACAAG  60
Obt.    CGCCATTCTGCCTGGGGACGTCGGAGCTAGCTTGATTTAGGTGACACTATAGAATACAAG  60
        ************************************************************

                                        S1
A.A.              M  V  F  T  N  E  F  E  Y  T  G  Y  L  V  V  L  M  S
Expec.  CTTACCATGGTCTTCACAAATGAATTTGAATATACTGGATACCTTGTGGTATTAATGAGC 120
Obt.    CTTACCATGGTCTTCACAAATGAATTTGAATATACTG---------------------- 98
        ***********************************

A.A.    T  Y  P  M  I  I  C  W  I  S  R  L  K  D  I  Y  D  N  E  I
Expec.  ACATATCCTATGATAATCTGTTGGATTTCCCGACTAAAAGACATCTATGACAACGAGATA 180
Obt.    ------------------------------------------------------------ 99
              S2
A.A.     K  C  A  N  Y  Y  F  L  A  F  Y  I  L  E  A  L  L  K  V  A
Expec.  AAGTGTGCTAACTACTATTTTCTTGCCTTCTATATTCTAGAGGCTCTACTTAAGGTGGCA 240
Obt.    ------------------------------------------------------------ 100
                       S3
A.A.    A  M  R  K  E  F  F  S  H  T  W  L  L  F  E  L  G  I  T  L
Expec.  GCAATGAGGAAGGAATTTTTTTCACACACCTGGCTCCTGTTTGAGCTGGGGATTACCTTA 300
Obt.    ------------------------------------------------------------ 100

A.A.    V  G  V  L  D  I  I  L  I  E  T  D  S  I  S  Y  N  F  D  L
Expec.  GTCGGCGTCCTAGATATAATACTTATCGAAACAGACTCCATTAGTTACAATTTTGACTTA 360
Obt.    ------------------------------------------------------------ 100
           S4
A.A.     T  E  T  V  V  F  M  N  V  I  R  L  L  R  I  L  R  I  L  K
Expec.  ACTGAGACTGTGGTCTTCATGAACGTGATTCGACTCCTTCGTATACTGCGCATCTTGAAG 420
Obt.    ----------------------------------------------CGATCTTGAAG 108
                                                      *********

A.A.    L  V  T  P  K  L  L
Expec.  CTAGTAACACCAAAACTACTGGGGGATCCCATGAGTAAAGGAGAAGAACTTTTCACTGGA 480
Obt.    CTAGTAACACCAAAACTACTGGGGGATCCCATGAGTAAAGGAGAAGAACTTTTCACTGGA 168
        ************************************************************
```

Figure S6. Problems in pCS2+-msNHE$_{VSD}$-pHluorin preparation. (A) Electrophoresis pattern of PCR19 (19F and 19R primers, Supplementary Table1) products (Lanes 1-2 and 3-6) from six putative pCS2+-msNHE$_{VSD}$-pHluorin plasmid obtained from different bacterial colonies. Lane M corresponds to DNA markers. The expected size of the PCR19 (Table S1) product was 1,458 bp (arrow). (B) Sequences of expected amino acid (A.A.), expected DNA (Exp.) and obtained DNA (Obt.) are shown. Identical DNA sequences were indicated by asterisks. Four boxes indicate putative transmembrane domain (S1-S4) of VSD of mouse sNHE. The DNA region encoding S1-S3 is missing in the obtained plasmid.

Fig. S7

A

MVFTNEFEYTGYLVVLMSTYPMIICWISRLKDIYDNEIKCAN
YYFLAFYILEALLKVAAMRKEFFSHTWLLFELGITLVGILDI
ILIETDSISYNFDLTETVVFMNVIRLLRILRILKLVTPKLL

B

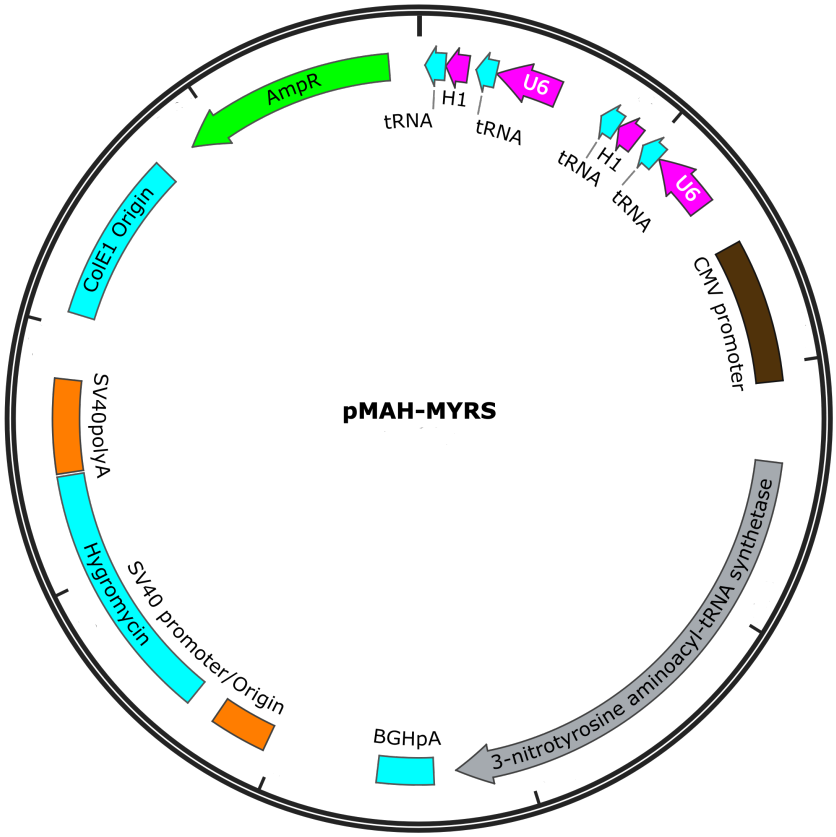

C

```
  1 MASSNLIKQL QERGLVAQVT DEEALAERLA QGPIALLCGF DPTADSLHLG HLVPLLCLKR
 61 FQQAGHKPVA LVGGATGLIG DPSFKAAERK LNTEETVQEW VDKIRKQVAP FLDFDCGENS
121 AIAANNYDWF GNMNVLTFLR DIGKHFSVNQ MINKEAVKQR LNREDQGISF TEFSYNLLQG
181 YDFACLNKQY GVVLSIGGSD QWGNITSGID LTRRLHQNQV FGLTVPLITK ADGTKFGKTE
241 GGAVWLDPKK TSPYKFYQFW INTADADVYR FLKFFTFMSI EEINALEEED KNSGKAPRAQ
301 YVLAEQVTRL VHGEEGLQAA KRITECLFSG SLSALSEADF EQLAQDGVPM VEMEKGADLM
361 QALVDSELQP SRGQARKTIA SNAITINGEK QSDPEYFFKE EDRLFGRFTL LRRGKKNYCL
421 ICWK
```

Figure S7. Amino acid sequence of msNHE$_{VSD}$ and Amber suppression plasmid, pMAH-MYRS. (A) Amino acid sequence of msNHE$_{VSD}$ used in this study. Underlines indicate the predicted transmembrane segments. Tyr665 where stop codon (TAG) was inserted is described with a red letter. Blue letters (KE) indicate a region where we inserted a synthetic small intron. (B) A map of pMAH-MYRS. The plasmid contains a 3-nitrotyrosine(3-NY)-aminoacyl-tRNA synthetase and four copies of its corresponding tRNA that recognizes UAG codon. (C) Amino acid sequence of the 3-NY-aminoacyl-tRNA synthetase encoded in pMAH-MYRS. The modified enzyme has only two mutations (Y37L/Q195S described in red letters) compared to the wild type enzyme.

Fig. S8

A

```
ATGGTCTTCACAAATGAATTTGAATATACTGGATACCTTGTGGTATTAATGAGCACATATCCTATGATAATCTGTTGGATTTCCCGACTA 90
AAAGACATCTATGACAACGAGATAAAATGTGCTAACTACTATTTTCTTGCCTTCTATATTCTAGAGGCTCTACTTAAGGTGGCAGCAATG 180
AGGAAGGTAAGTATCAAGGTTACAAGACAGGTTTAAGGAGACCAATAGAAACTGGGCTTGTCGAGACAGAGAAGACTCTTGCGTTTCTGA 270
TAGGCACCTATTGGTCTTACTGACATCCACTTTGCCTTTCTCTCCACAGGAATTTTTTTCACACACCTGGCTCCTGTTTGAGCTGGGGAT 360
TACCTTAGTCGGCATCCTAGATATAATACTTATCGAAACAGACTCCATTAGTTACAATTTTGACTTAACTGAGACTGTGGTCTTCATGAA 450
CGTGATTCGACTCCTTCGTATACTGCGCATCTTGAAGCTAGTAACACCAAAACTACTGGGGGATCCCATGAGTAAAGGAGAAGAACTTTT 540
CACTGGAGTTGTCCCAATTCTTGTTGAATTAGATGGTGATGTTAATGGGCACAAATTTTCTGTCAGTGGAGAGGGTGAAGGTGATGCAAC 630
ATACGGAAAACTTACCCTTAAATTTATTTGCACTACTGGAAAACTACCTGTTCCATGGCCAACACTTGTCACTACTTTAACTTATGGTGT 720
TCAATGCTTTTCAAGATACCCAGATCATATGAAACGGCATGACTTTTTCAAGAGTGCCATGCCCGAAGGTTATGTACAGGAAAGAACTAT 810
ATTTTTCAAAGATGACGGGAACTACAAGACACGTGCTGAAGTCAAGTTTGAAGGTGATACCCTTGTTAATAGAATCGAGTTAAAAGGTAT 900
TGATTTTAAAGAAGATGGAAACATTCTTGGACACAAATTGGAATACAACTATAACGATCACCAGGTGTACATCATGGCAGACAAACAAAA 990
GAATGGAATCAAAGCTAACTTCAAAATTAGACACAACATTGAAGATGGAGGCGTTCAACTAGCAGACCATTATCAACAAAATACTCCAAT 1080
TGGCGATGGGCCCGTCCTTTTACCAGACAACCATTACCTGTTTACAACTTCTACTCTTTCGAAAGATCCCAACGAAAAGAGAGACCACAT 1170
GGTCCTTCTTGAGTTTGTAACAGCTGATGGGATTACACATGGCATGGATGAACTATACAAATGA 1234
```

B

```
MVFTNEFEYTGYLVVLMSTYPMIICWISRL 30
KDIYDNEIKCANYYFLAFYILEALLKVAAM 60
RKEFFSHTWLLFELGITLVGVLDIILIETD 90
SISYNFDLTETVVFMNVIRLLRILRILKLV 120
TPKLLGDPMSKGEELFTGVVPILVELDGDV 150
NGHKFSVSGEGEGDATYGKLTLKFICTTGK 180
LPVPWPTLVTTLTYGVQCFSRYPDHMKRHD 210
FFKSAMPEGYVQERTIFFKDDGNYKTRAEV 240
KFEGDTLVNRIELKGIDFKEDGNILGHKLE 270
YNYNDHQVYIMADKQKNGIKANFKIRHNIE 300
DGGVQLADHYQQNTPIGDGPVLLPDNHYLF 330
TTSTLSKDPNEKRDHMVLLEFVTADGITHG 360
MDELYK* 366
```

Figure S8. DNA and amino acid sequences of pCS2+-VSD$_{Intron}$-pHluorin. DNA (A) and amino acid (B) sequences of pCS2+-VSD$_{Intron}$-pHluorin are described with distinct colors corresponding to each fragments. Color codes: msNHE$_{VSD}$ (orange), Intron (gray), GDP amino acids from BamHI site (originally for Arclight; black), pHluorin (green).

Fig. S9

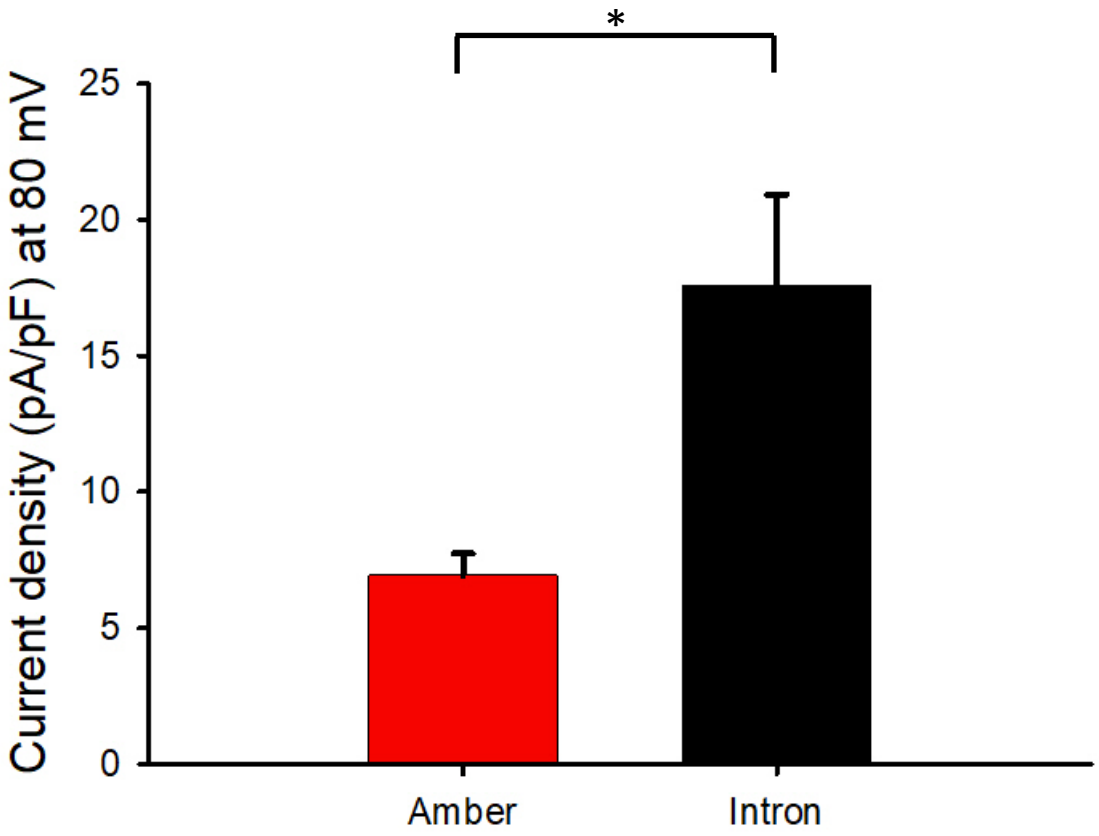

Figure S9. Outward current densities of HEK293 cells transfected with two constructions containing msNHE$_{VSD}$. The mean current densities (± S.D.) of the outward current of the two constructions are shown. Amber (red): transfected with pCS2+-VSD$_{Y665Amber}$-pHluorin and pMAH-MYRS (n = 5). Intron (black): transfected with pCS2+-VSD$_{Intron}$-pHluorin (n = 5). * significant difference ($p<0.05$).